Nanometric Phase Transitions on Phospholipid Membranes Using Plasmonic Heating of Single Gold Nanoparticles

ARTICLE *in* NANO LETTERS · SEPTEMBER 2009

Impact Factor: 13.59 · DOI: 10.1021/nl901201h · Source: PubMed

6 AUTHORS, INCLUDING:

Alexander Urban
Ludwig-Maximilians-University of Munich
29 PUBLICATIONS **688** CITATIONS
SEE PROFILE

Fernando D. Stefani
National Scientific and Technical Research…
48 PUBLICATIONS **2,045** CITATIONS
SEE PROFILE

NANO LETTERS

2009
Vol. 9, No. 8
2903-2908

Controlled Nanometric Phase Transitions of Phospholipid Membranes by Plasmonic Heating of Single Gold Nanoparticles

A. S. Urban,[†] M. Fedoruk,[†] M. R. Horton,[‡] J. O. Rädler,[‡] F. D. Stefani,*[,†] and J. Feldmann*[,†]

Photonics and Optoelectronics Group, Fakultät für Physik and CeNS, Ludwig-Maximilians-Universität München, Amalienstrasse 54, 80799 Munich, Germany, and Soft Condensed Matter Group, Fakultät für Physik and CeNS, Ludwig-Maximilians-Universität München, Geschwister-Scholl Platz-1, 80799 Munich, Germany

Received April 15, 2009; Revised Manuscript Received May 20, 2009

ABSTRACT

The development of remotely controlled nanoscopic sources of heat is essential for investigating and manipulating temperature sensitive processes at the nanoscale. Here, we use single gold nanoparticles to rapidly deposit controlled amounts of heat in nanoscopic regions of defined size. This allows us to induce and control nanoscale reversible gel-fluid phase transitions in phospholipid membranes. We exploit the optical control over the phase transition to determine the velocity of the fluid phase front into the gel phase membrane and to guide the nanoparticles to specific locations. These results illustrate how single gold nanoparticles enable local thermodynamic investigation and manipulation on nanoscale (bio-) systems.

Impressive advances have recently been made in imaging structural properties of cellular and subcellular systems[1,2] and in visualizing their pathways[3,4] by optical techniques with nanometric resolution. Full understanding of these systems requires additional information on the dynamics and energy of the molecular interactions involved. This information has been traditionally obtained by bulk calorimetry techniques.[5,6] Metallic nanoparticles can be efficiently heated by illuminating them at their plasmon resonances.[7,8] In recent years, this optical heating has found a number of applications including remote release,[9] microscopy,[10] biomolecular analysis,[11] and even as a prospect for cancer therapy by destroying biological cells.[12] However, the full potential of metallic nanoparticles to heat nanoscopic portions of matter, thereby providing nanoscale local information and control capabilities, remains largely unexplored. In this work, we combine optical (plasmonic) heating, single particle tracking, and finite element calculations to demonstrate the use of single gold nanoparticles for nanoscale thermodynamic investigation and manipulation on phospholipid membranes. The nanoparticles simultaneously induce and characterize the gel-fluid phase transition of the membrane in defined nanometric regions.

Many vital processes such as photosynthesis, cellular respiration, signal transduction as well as endo- and exocytosis take place in cellular or subcellular membranes.[13] Even though biological membranes vary considerably in their composition, their basic structural unit is the phospholipid bilayer.[13] Pure phospholipid bilayer membranes exhibit a sharp thermal transition between a gel and a fluid phase. Below the melting temperature (T_m), the membrane is in the gel phase where the phospholipids are bound tightly together by van der Waals forces between their acyl chains. Above T_m, the intermolecular interaction between phospholipids is reduced. In this fluid phase, the mobility of phospholipids within the membrane is typically 2 orders of magnitude higher than in the gel phase.[14] The value of T_m depends on the lipid composition of the membrane; double bonds in the acyl chains as well as shorter acyl chains cause lower transition temperatures. The presence of cholesterol in biological membranes makes a different kind of phase possible: the liquid-ordered phase. In this phase, the acyl chains are extended and tightly packed, as in the gel phase, but have a high degree of lateral mobility.[15] The membrane

* To whom correspondence should be addressed. E-mail: (F.D.S.) fernando.stefani@physik.uni-muenchen.de; (J.F.) jochen.feldmann@physik.uni-muenchen.de.

[†] Photonics and Optoelectronics Group, Fakultät für Physik and CeNS, Ludwig-Maximilians-Universität München.

[‡] Soft Condensed Matter Group, Fakultät für Physik and CeNS, Ludwig-Maximilians-Universität München.

10.1021/nl901201h CCC: $40.75
Published on Web 07/07/2009

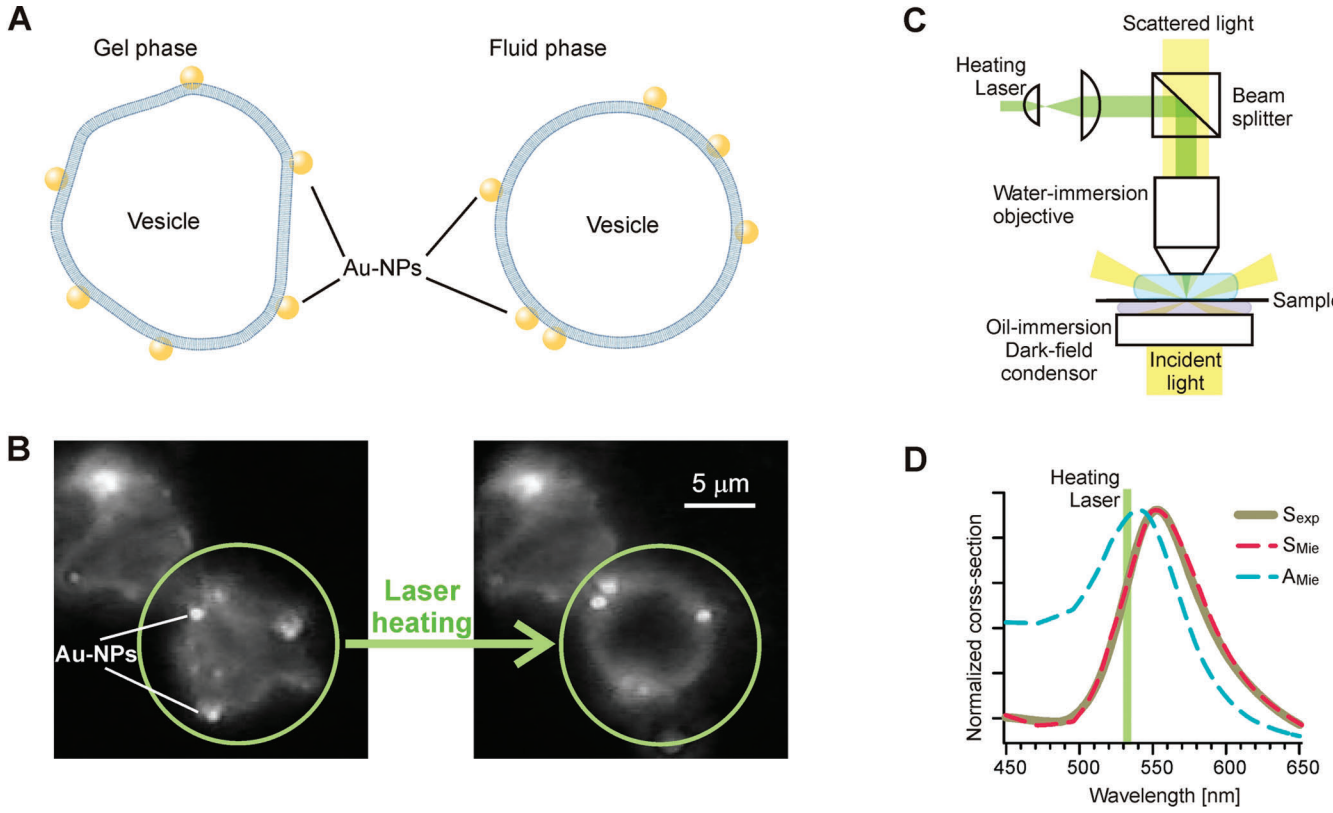

Figure 1. Optically induced phase transition of a nanoparticle-modified giant unilamellar vesicle. (A) Schematic of a vesicle in the gel (left) and in the fluid (right) phase modified with gold nanoparticles (Au-NPs). For clarity, the schematics are not drawn to scale (the phospholipid membrane has a thickness of 5 nm and the gold nanoparticles a diameter of 80 nm). (B) Dark-field micrograph of two adjacent gel-phase vesicles modified with gold nanoparticles (left). Membrane and nanoparticles appear with a size of about 1 μm due to the diffraction limited detection of the scattering signal. The brightness scale is saturated in order to visualize both the strongly scattering gold nanoparticles and the weakly scattering phospholipid membrane. The lower vesicle is illuminated with the heating laser (green circle) for about 1 min with a power density $P \cong 100$ kW/cm^2. This vesicle relaxes to a spherical shape (right). (C) Dark-field microscope adapted for optical heating. (D) Calculated (Mie theory) absorption (A_{Mie}) and scattering (S_{Mie}) spectra together with the measured scattering spectrum (S_{exp}) of an 80 nm gold nanoparticle. A vertical line marks the 532 nm wavelength of the heating laser.

phase of a biological cell is thought to influence or regulate a number of processes including protein partitioning and endocytotic trafficking.[15,16]

Artificial model membranes have played an important role in revealing physical and chemical characteristics of membrane function.[17,18] We used phospholipid giant unilamellar vesicles (GUVs; 15 to 50 μm in diameter) prepared by electroformation[19] as a model system for the biological cell membrane. Vesicles in the gel phase generally present faceted shapes due to the rigidity of the membrane, whereas vesicles in the fluid phase take a spherical shape (Figure 1A). Gold nanoparticles with a diameter of 80 nm were coated with cetyl trimethyl ammonium bromide (CTAB) and attached to the surface of the vesicles (Figure 1B). We used optical dark-field microscopy (Figure 1C) to characterize the nanoparticle-modified vesicles, to perform spectroscopy on the gold nanoparticles, and to directly visualize the effects of nanoparticle heating. A continuous-wave (heating) laser at 532 nm was used to illuminate the nanoparticles near their plasmon resonance (Figure 1C,D). We observed that in comparison to gold nanoparticles with other surface ligands (e.g., citrate molecules) the CTAB-coated nanoparticles have a considerably higher affinity to the phospholipid membranes. The precise origin of this interaction is not fully understood. However, a strong interaction between the CTAB and phospholipid molecules is indicated by the observation that the gold nanoparticles are immobile when attached to vesicles in the gel phase.

In a first experiment, gold nanoparticles were attached to 1,2-dipalmitoyl-sn-glycero-3-phosphocholine (DPPC) vesicles, which have a T_m of 41 °C[14] and are therefore in the gel phase at room temperature (Figure 1B). We optically heated the gold nanoparticles with power densities $P < 350$ kW/cm^2. Higher values of P led to the destruction of the vesicles. Figure 1B shows the effect of the simultaneous optical heating of several gold nanoparticles attached to a DPPC vesicle. Within a short period of time the illuminated vesicle relaxed into the energetically favorable spherical shape. In addition, during the optical heating, the beforehand immobile nanoparticles started to move over the membrane.[20] Laser illumination at 633 nm, where the gold nanoparticles do not absorb substantially, produced no effect.

In order to understand the light-induced heat deposition and the behavior of the nanoparticle-modified vesicles, we simulated the heat transfer in our system by finite-element calculations. These calculations require the absorption cross-section of the gold nanoparticle, the laser power density, the geometry of the nanoparticle-membrane system, and the

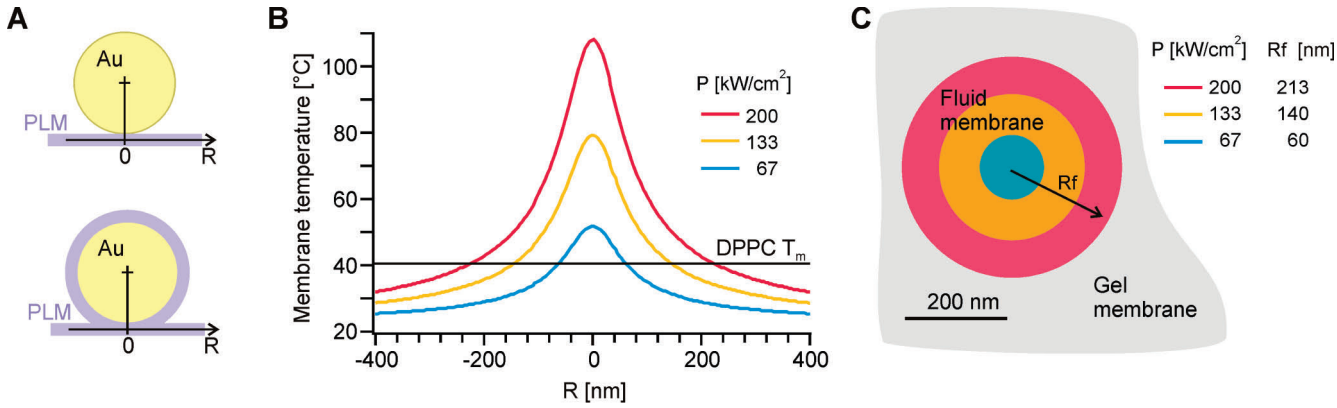

Figure 2. Local nanometric heating of phospholipid membranes by gold nanoparticles. (A) Geometries of the nanoparticle-membrane system used in the heat transfer finite element calculations. The phospholipid membrane (PLM) is 5 nm thick, and the gold nanoparticle has a diameter of 80 nm. (B) Steady-state temperature at the center of the horizontal membrane as a function of the distance R to the nanoparticle center for three power densities P of the heating laser. The horizontal line marks the gel-fluid phase transition temperature T_m for DPPC. (C) Circular regions of the DPPC membrane around the gold nanoparticle position reach a temperature above T_m. The radius of the fluid region (Rf) increases with the power density of the heating laser.

thermal capacity and conductivity of all components. We determined the absorption cross-section from experimentally measured scattering spectra (Figure 1D). We used standard values for the thermal properties of gold and of the surrounding solution. The extent to which the membrane bends around the gold nanoparticle is not known.[21] We therefore simulated the two extreme situations of a nanoparticle lying over a flat membrane and of a nanoparticle fully wrapped by the membrane (Figure 2A). Since the thermal conductivity of phospholipid membranes is also unknown, we performed calculations using a range of values from those of hydrocarbons of similar acyl chains to those of common polymers. Likewise, the heat capacity was varied by an order of magnitude around reported values.[22,23] It turns out that the thermal properties of the membrane as well as the degree of wrapping only have a small influence on the thermal behavior of the full system. The variation of these parameters produces temperature deviations of 2−8% only in the close proximity of the gold nanoparticle ($R < 20$ nm, Figure 2A). Illumination with the heating laser results in a highly localized temperature increase around the nanoparticle (Figure 2B). In such small nanometric regions, water can reach temperatures above 100 °C without boiling.[24] A defined circular region of the membrane around the nanoparticle is hotter than T_m (Figure 2C). The radius of this fluid region (Rf) increases with P and lies in the 0−350 nm range. The heating of the phospholipid membrane is extremely rapid; 95% of the steady-state temperature is typically reached within 100 ns. These calculations explain the experimental observations. Gold nanoparticles free in solution undergo three-dimensional Brownian motion. On the surface of a gel membrane, the nanoparticle motion is stopped as a result of the low mobility of the phospholipids in the membrane and the strong interaction of CTAB and phospholipid molecules. When optically heated, the gold nanoparticles melt a region of radius Rf in the vesicle membrane. The much higher lipid mobility in the surrounding fluid region re-enables the nanoparticle motion, this time in two dimensions over the membrane surface. The nanoparticles melt other regions as they move. Because of the nearly Gaussian intensity profile of the illumination spot, Rf decreases outward from the center. The nanoparticle movement is therefore limited to a membrane corral imposed by Rf > 0 (Figure 3A).

To analyze the increased mobility of the optically heated nanoparticles upon membrane melting, we recorded their motion on video. DPPC vesicles with at least three gold nanoparticles were used. Only one nanoparticle was optically heated at any given time (Figure 3B). These nanoparticles moved over the area of illumination and stopped, concomitantly with successive switching on and off of the heating laser.[20] Within the illumination area, the nanoparticle movement was fastest in the center, where Rf and the power density are maximal (P_{max}) (Figure 3B). Away from the center, the nanoparticles were slower and eventually stopped altogether. Increasing the laser intensity led to an overall faster movement and to a larger diffusion corral. The (two) nanoparticles outside the heating laser spot remained immobile throughout the entire measurement. We tracked the nanoparticle positions (Figure 3B) in the form of a time sequence $[x_n = x(n\Delta T), y_n = y(n\Delta T)]$ with $n = 0, 1, 2...N$ being the video frame number and ΔT is the data acquisition time given by the video frame rate (33 ms). Recording the positions of the two immobile nanoparticles allowed us to subtract movements of the vesicle as a whole. From the recorded trajectories we calculated the time dependent mean square displacement (MSD)

$$\mathrm{MSD}(t) = \mathrm{MSD}(n\Delta T) = \frac{1}{N+1}\sum_{i=0}^{N}(x_{i+n} - x_i)^2 + (y_{i+n} - y_i)^2$$

For free two-dimensional diffusion, $\mathrm{MSD}(t) = 4Dt$, where D is the diffusion coefficient.[25] Four examples of MSD(t) are shown in Figure 3C for different values of P_{max}. For low values of P_{max}, the nanoparticles diffused freely within the corral imposed by the heating spot, as shown by the linear dependence of MSD(t). D increased with higher P_{max} as

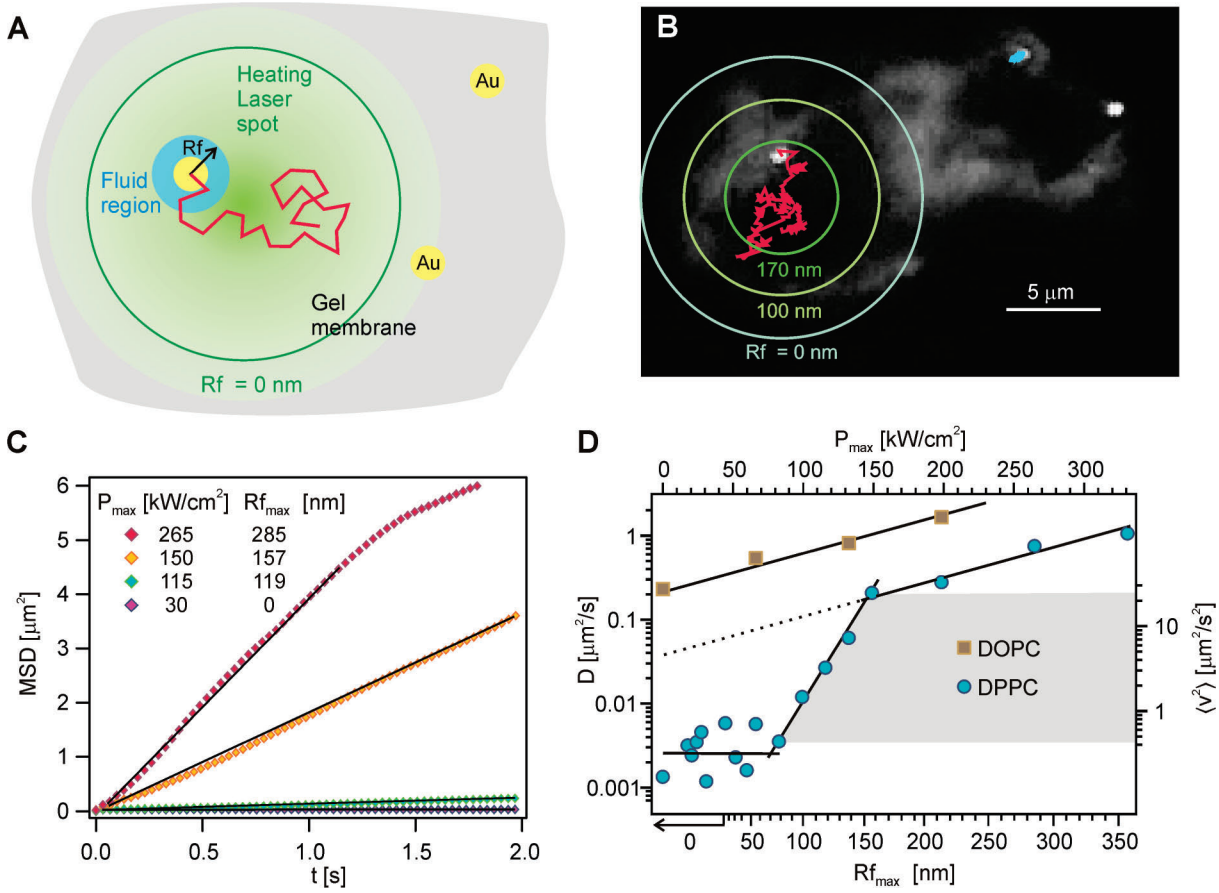

Figure 3. Nanometric gel-fluid phase transitions of phospholipid membranes. (A) An optically heated gold nanoparticle melts a region of the membrane with radius Rf and may move over the membrane. For a Gaussian heating spot, Rf decreases outward from the center. The heated nanoparticle movement is restricted to the area where Rf > 0. (B) Dark-field micrograph of a gel phase DPPC vesicle with three gold nanoparticles on its surface. Only the nanoparticle on the left is optically heated. A 10 s trajectory of this nanoparticle (red; Pmax = 200 kW/cm^2) and of one of the nonheated nanoparticles (light blue) are shown. The green circles denote the calculated radius Rf of the fluid region around the heated nanoparticle for different positions within the illumination area (Gaussian, 9 μm fwhm). (C) MSD vs time of gold nanoparticles on a DPPC vesicle for four values of P_{max} (Rf_{max}). (D) Diffusion coefficient D and mean square velocity $\langle v^2 \rangle$ of gold nanoparticles on the surface of DPPC and DOPC vesicles as a function of P_{max} (Rf_{max}). Each value of D is the average obtained from at least 10 nanoparticle trajectories. The statistical error bars are smaller than the plot markers.

reflected in the larger slopes of MSD(t). For sufficiently high P_{max} (e.g., P_{max} = 265 kW/cm^2) the gold nanoparticles exhibited a subdiffusive behavior. This is a result of their mobility being so high that within the observation time the gold nanoparticles reached the limits of the diffusion corral.

We obtained further insight into the nanoscale phase transition by measuring the diffusion coefficient of nanoparticles on DPPC and 1,2-dioleoyl-sn-glycero-3-phosphocholine (DOPC) vesicles as a function of P_{max} (Figure 3D). The membranes of DOPC have a T_m of approximately −20 °C[14] and are thus in the fluid phase at room temperature. Measurements on DOPC vesicles serve as a control for the influence of optical heating on the mobility of gold nanoparticles on a fluid phospholipid membrane. Gold nanoparticles on DOPC vesicles display an exponential increase of D with P_{max} (Figure 3D), reflecting the reduction of the fluid membrane viscosity with temperature. The values of D correspond well to reported diffusion coefficients of lipid-tagged gold nanoparticles on fluid artificial bilayers[26] and biological membranes.[27] In contrast, measurements on DPPC vesicles reveal three different regimes of D as a function of P_{max} (Figure 3D). In the high P_{max} regime, an exponential dependence analogous to the one of gold nanoparticles on DOPC is observed. For a given P_{max}, the viscosity of the fluid DPPC membrane is higher than that of a DOPC membrane due to the lower relative temperature ($T - T_m$). Thus, the values of D for nanoparticles on DPPC are lower than for DOPC. In the intermediate regime, D exhibits a substantially faster exponential increase than in the high P_{max} regime. And in the low P_{max} regime, nanoparticle movement is undetectable. The scatter of the data for P_{max} < 80 kW/cm^2 results from the experimental error of 150 nm in the localization of the nanoparticles. In order to understand these results, we need to account for the dynamics of the phase transition. The nanoparticle heats up a region of radius Rf to a temperature above T_m on a submicrosecond time scale. However, the complete melting of that region may take considerably longer. In the high P_{max} regime, the nanoparticles are extremely hot. The fluid region around them is generated so rapidly that they diffuse freely as the nanoparticles on the full fluid membranes of DOPC do. In the intermediate regime, the movement of the nanoparticle is

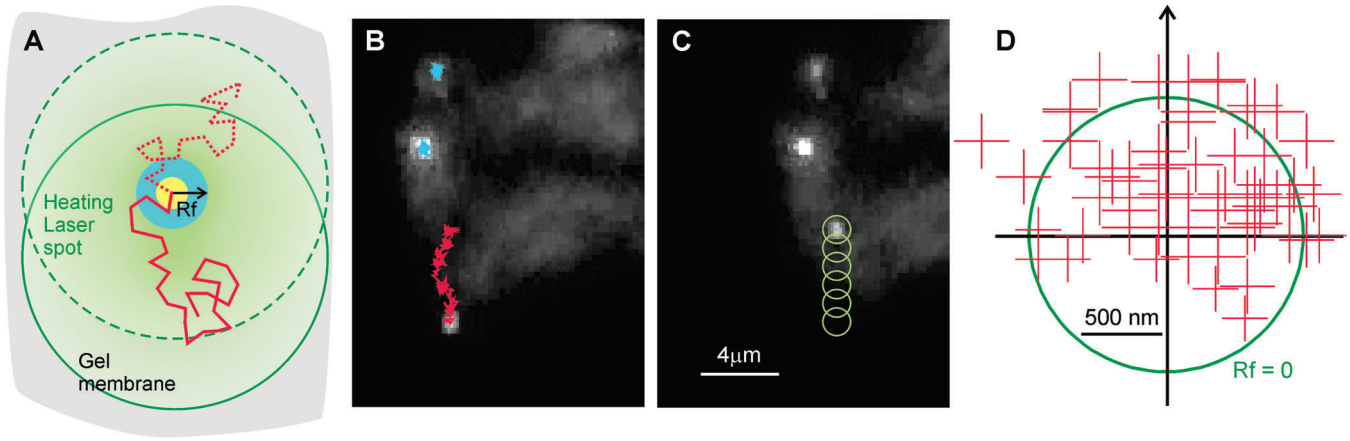

Figure 4. Guided motion of optically heated nanoparticles over a membrane in the gel phase. (A) The nanoparticle may follow the heating laser spot if the latter is moved at a rate comparable to the time the nanoparticle needs to explore the diffusion corral. (B) First frame of the video recording of a guided motion experiment. The trajectory of the guided nanoparticle is shown in red and of the reference nanoparticles in light blue. (C) Last frame of the video. The trajectory of the laser heating spot is schematically shown to scale. (D) Positions of guided nanoparticles relative to the heating laser spot during the guiding process. The arrow indicates the guiding direction and the circle the calculated limit for membrane melting.

limited by the rate of the phase transition. A gold nanoparticle moving along the membrane cannot progress faster than the fluid front advances from the hot nanoparticle surface into the gel phase. In this regime the velocity of the fluid phase front is directly obtained from the relation $\langle v^2 \rangle = D/\Delta T$[25] (Figure 3D, right axis). We determine fluid phase front velocities ranging from 0.9 to 4.5 μm/s. In the low P_{max} regime, either the heat produced by the gold nanoparticle is not sufficient to produce a fluid region or the time needed by the fluid front to advance is too long to enable a noticeable nanoparticle motion.

The potential of single gold nanoparticles as thermal nanotools is further enhanced if they can be positioned at specific locations on the membrane. One way to achieve this is to exploit the optical control of the local phase transition. We took advantage of the fact that a hot nanoparticle undergoes corralled diffusion with limits determined by the intensity profile of the heating laser to direct them over the membrane surface. If the heating spot is displaced with a rate comparable to the time needed by the nanoparticle to explore the diffusion corral, the nanoparticle may follow the displacement of the heating spot (Figure 4A). Again, we used DPPC vesicles with at least three nanoparticles attached to the membrane and heated only one nanoparticle. The heating spot was focused (0.9 μm fwhm) in order to confine the lateral motion of the gold nanoparticles and displaced in a certain direction. The hot gold nanoparticle followed the heating spot (red trace, Figure 4B,C) while the other two nanoparticles remained immobile (light blue, Figure 4B). Since the heating beam was focused and tuned to the plasmon resonance, the gold nanoparticles tended to be expelled from the center of the heating spot by optical forces.[28] Effective guiding was consequently achieved by driving the gold nanoparticles from behind in the desired direction; that is, the gold nanoparticles stayed in the front half of the laser spot (Figure 4D). Although during the guided motion the gold nanoparticles diffused laterally within the limits imposed by the heating spot, it is possible to position them with nm precision. Once the desired position is reached, the laser spot is expanded to decrease the optical forces. Then, the laser intensity is gradually reduced, progressively confining the nanoparticle to a smaller region near the laser spot center.

In summary, these results illustrate the use of single gold nanoparticles for local nanoscale thermodynamic investigations on phospholipid membranes. First, we demonstrated the controlled application of heat around the nanoparticles by inducing the reversible gel-fluid phase transition of nanometric regions of the membrane. Second, we showed how the size of the fluid region and the mobility of nanoparticles over the membrane surface are regulated by the power density of the heating laser. Furthermore, the nanoparticle motion reveals local information on the dynamics of the phase transition. That allowed us to determine the velocity with which the fluid phase front advances. Finally, we used the ability to optically control the phase transition to guide nanoparticles to specific locations on the membrane.

Optically controlled nanoscopic sources of heat may find wide application. The extensive knowledge of surface functionalization of metallic nanoparticles should enable their use for nanoscale investigation and manipulation of temperature sensitive processes in artificial as well as biological systems. Metallic nanoparticles of different sizes, compositions, and shapes may be used to achieve larger absorption cross sections and to tune the resonant absorption into various spectral windows. This may be essential to avoid unwanted photoinduced damage or reactions in biological systems. The approach presented here can be easily extended by combining it with other microscopy methods and optical tweezer techniques.

Acknowledgment. This work has been supported by the German Excellence Initiative of the Deutsche Forschungsgemeinschaft (DFG) via the "Nanosystems Initiative Munich (NIM)".

Supporting Information Available: This material is available free of charge via the Internet at http://pubs.acs.org.

References

(1) Nagerl, U. V.; Willig, K. I.; Hein, B.; Hell, S. W.; Bonhoeffer, T. *Proc. Natl. Acad. Sci. U.S.A.* **2008**, *105* (48), 18982–18987.
(2) Huang, B.; Wang, W. Q.; Bates, M.; Zhuang, X. W. *Science* **2008**, *319* (5864), 810–813.
(3) Yildiz, A.; Forkey, J. N.; McKinney, S. A.; Ha, T.; Goldman, Y. E.; Selvin, P. R. *Science* **2003**, *300* (5628), 2061–2065.
(4) Lidke, D. S.; Nagy, P.; Heintzmann, R.; Arndt-Jovin, D. J.; Post, J. N.; Grecco, H. E.; Jares-Erijman, E. A.; Jovin, T. M. *Nat. Biotechnol.* **2004**, *22* (2), 198–203.
(5) Weber, P. C.; Salemme, F. R. *Current Opinion in Structural Biology* **2003**, *13* (1), 115–121.
(6) Leavitt, S.; Freire, E. *Curr. Opin. Struct. Biol.* **2001**, *11* (5), 560–566.
(7) Richardson, H. H.; Carlson, M. T.; Tandler, P. J.; Hernandez, P.; Govorov, A. O. *Nano Lett.* **2009**, *9* (3), 1139–1146.
(8) Perner, M.; Gresillon, S.; Marz, J.; von Plessen, G.; Feldmann, J.; Porstendorfer, J.; Berg, K. J.; Berg, G. *Phys. Rev. Lett.* **2000**, *85* (4), 792–795.
(9) Skirtach, A. G.; Dejugnat, C.; Braun, D.; Susha, A. S.; Rogach, A. L.; Parak, W. J.; Mohwald, H.; Sukhorukov, G. B. *Nano Lett.* **2005**, *5* (7), 1371–1377.
(10) Cognet, L.; Tardin, C.; Boyer, D.; Choquet, D.; Tamarat, P.; Lounis, B. *Proc. Natl. Acad. Sci. U.S.A.* **2003**, *100* (20), 11350–11355.
(11) Stehr, J.; Hrelescu, C.; Sperling, R. A.; Raschke, G.; Wunderlich, M.; Nichtl, A.; Heindl, D.; Kurzinger, K.; Parak, W. J.; Klar, T. A.; Feldmann, J. *Nano Lett.* **2008**, *8* (2), 619–623.
(12) Hirsch, L. R.; Stafford, R. J.; Bankson, J. A.; Sershen, S. R.; Rivera, B.; Price, R. E.; Hazle, J. D.; Halas, N. J.; West, J. L. *Proc. Natl. Acad. Sci. U.S.A.* **2003**, *100* (23), 13549–13554.
(13) Lodish, H. F.; Darnell, J. E. *Molecular cell biology*, 3rd ed.; Scientific American Books: New York, 1995.
(14) Heimburg, T. *Thermal biophysics of membranes*; Wiley-VCH Verlag: Weinheim, 2007.
(15) Brown, D. A.; London, E. *J. Biol. Chem.* **2000**, *275* (23), 17221–17224.
(16) Rajendran, L.; Simons, K. *J. Cell Sci.* **2005**, *118* (6), 1099–1102.
(17) Chan, Y. H. M.; Boxer, S. G. *Curr. Opin. Chem. Biol.* **2007**, *11* (6), 581–587.
(18) Lipowsky, R.; Sackmann, E. *Structure and dynamics of membranes*; Elsevier Science: Amsterdam, 1995.
(19) Bagatolli, L. A.; Gratton, E. *Biophys. J.* **1999**, *77* (4), 2090–2101.
(20) See Supporting Information.
(21) Deserno, M.; Gelbart, W. M. *J. Phys. Chem. B* **2002**, *106* (21), 5543–5552.
(22) Blume, A. *Biochemistry* **1983**, *22* (23), 5436–5442.
(23) Gershfeld, N. L.; Mudd, C. P.; Tajima, K.; Berger, R. L. *Biophys. J.* **1993**, *65* (3), 1174–1179.
(24) Skripov, V. P.; Torstveit, S. *Thermophysical properties of liquids in the metastable (superheated) state*; Gordon and Breach Science Publishers: New York, 1988.
(25) Hong, Q. A.; Sheetz, M. P.; Elson, E. L. *Biophys. J.* **1991**, *60* (4), 910–921.
(26) Lee, G. M.; Ishihara, A.; Jacobson, K. A. *Proc. Natl. Acad. Sci. U.S.A.* **1991**, *88* (14), 6274–6278.
(27) Lee, G. M.; Zhang, F.; Ishihara, A.; Mcneil, C. L.; Jacobson, K. A. *J. Cell Biol.* **1993**, *120* (1), 25–35.
(28) Agayan, R. R.; Gittes, F.; Kopelman, R.; Schmidt, C. F. *Appl. Opt.* **2002**, *41* (12), 2318–2327.

NL901201H